239. Integration of Satellite Image and In-Situ Observations for Analysis of Meso-Gamma Scale Eddies in the Marine Stratocumulus Photographed by Pilots near the California Coast

Bradley M. Muller (bradley.muller@erau.edu)

Christopher G. Herbster (christopher.herbster@erau.edu)

Frederick R. Mosher (frederick.mosher@erau.edu)

Embry-Riddle Aeronautical University

600 S. Clyde Morris Blvd.

Daytona Beach, FL 32114-3900

http://wx.erau.edu

Aerial photograph of eddy near Santa Cruz Island 16 July 2006.

Fig. 1. Eddy north of Santa Cruz Island 18:26 UTC (11:26 PDT), July 16, 2006. Photo direction is toward the southwest. Santa Rosa Island is faintly visible in the background. (Photo by "KB" courtesy of Capt. Peter Weiss, SkyWest Airlines).

Aerial photograph of eddy over San Luis Bay (near Grover Beach and San Luis Obispo) 12 September 2006.

Fig. 4. Coastal eddy just west of Grover Beach, California, at approximately 18:28 UTC (11:28 PDT), September 12, 2006. Photo direction is toward the west. (Photo by "KB," courtesy of Capt. Peter Weiss)

GOES satellite images of formation of Santa Cruz Island eddy, 16 July 2006.

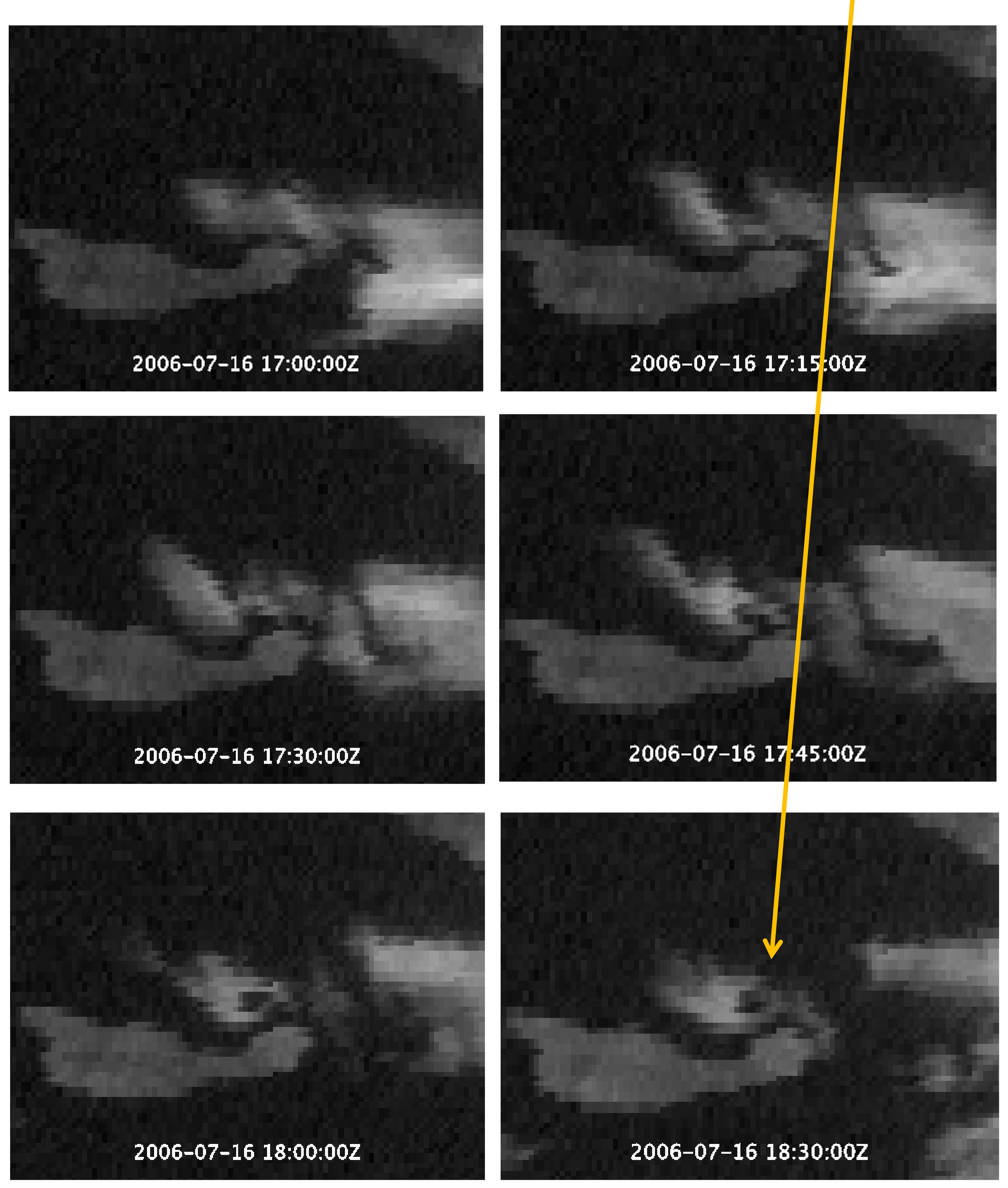

Fig. 2 GOES-West visible satellite images from 17:00 UTC to 18:30 UTC on July 16, 2006. In this sequence, dry, cloud-free, sinking air in the lee of Santa Cruz Island can be seen moving laterally into the circulation followed by a tongue of clouds wrapping around and closing off the "eye." The satellite image from 18:30 UTC shows the same cloud (orange arrow) as Figure 1. Analysis of this cloud indicates the width to be 9-10 km, length of 25 km, and cloud-free eye of 3 km.

GOES images of formation and movement of Grover Beach eddy, 12 September 2006.

Fig. 5 GOES-West images from Sept. 12, 2006. Superimposed are wind/temperature data from the Pacific Gas &Electric (PG&E) Co. network, from the Cal Poly (California Polytechnic State University, San Luis Obispo) pier, and wind data from the San Luis Obispo County Air Pollution Control (SLOAPCD) district. Half barbs represent wind speeds of 2.5 m s^{-1}. Whole barbs represent wind speeds of 5 m/s, and open circles represent wind speeds of less than 1.5 m/s. **Initially the eddy moves with the northeasterly above-inversion flow toward the southwest, then moves with the northwesterly and westerly marine boundary layer flow toward the east. These motions suggest an eddy initiating within the inversion layer then cross-inversion mixing down into the marine boundary layer. Circulations clearly extend down to surface.** The satellite image at 1830 UTC shows the same cloud as Figure 4 (orange arrrow). At 1830 UTC the eddy feature has a length of 17 km, width of 9 km, and cloud-free eye of 2.5-3 km.

Eddies appear similar to Von Karman vortices (e.g., Young and Zawislak 2006).

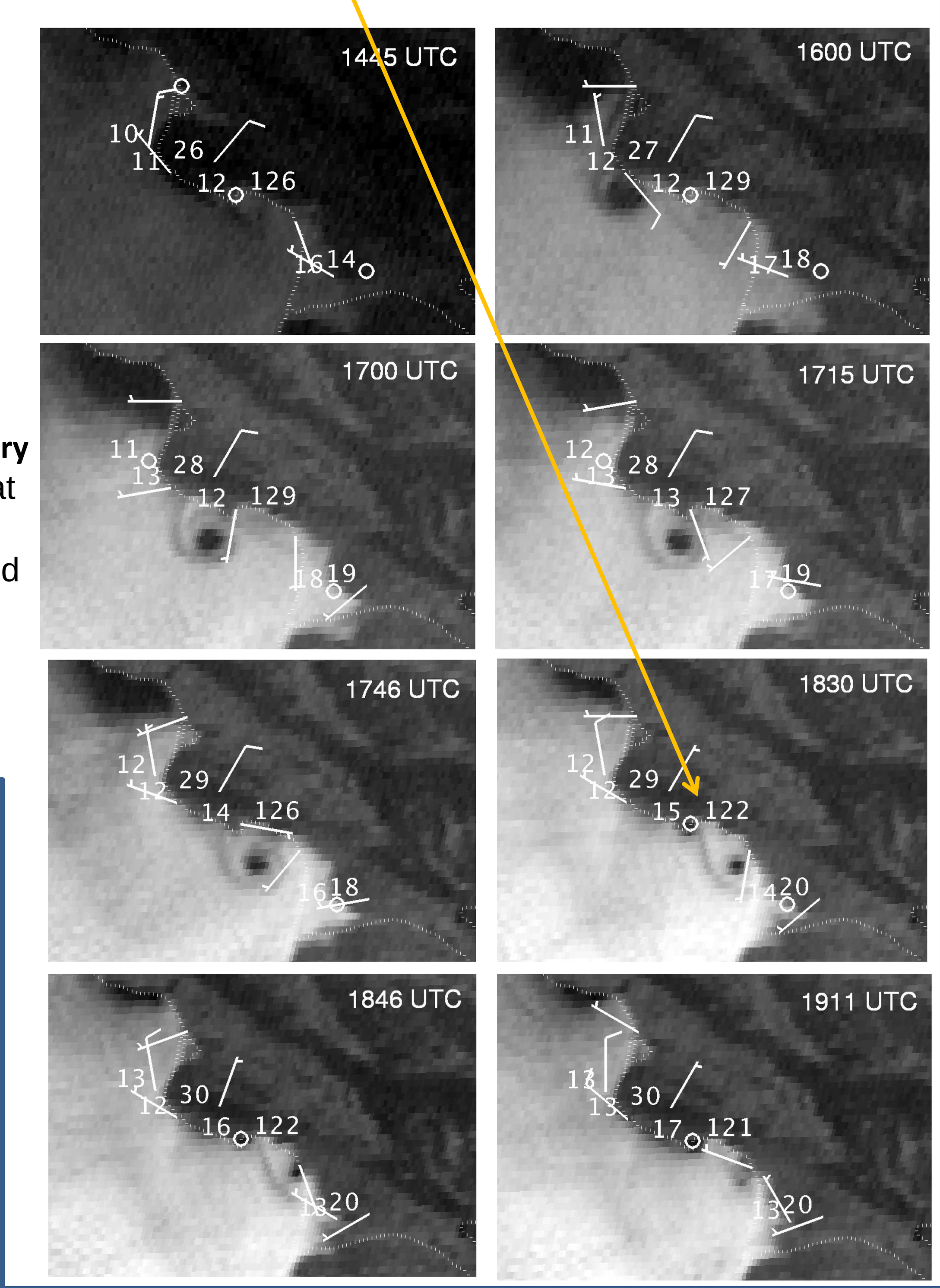

Terrain that produced the Grover Beach eddy.

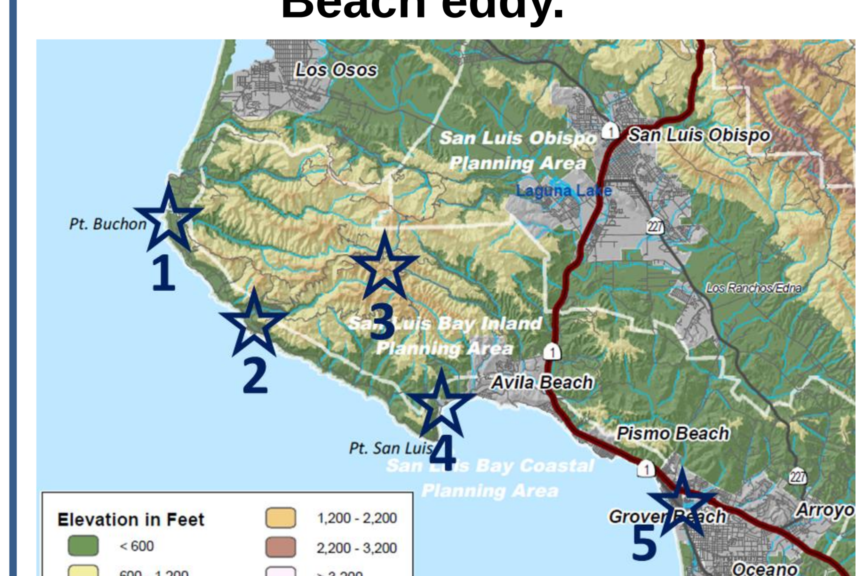

Fig. 6 Terrain that produced the Grover Beach eddy, with the locations of relevant monitoring stations superimposed and numbered as follows, PG&E 1-3: 1) Pt. Buchon 2) Diablo Canyon Nuclear Power Plant meteorological tower 3) Davis Peak; 4) Cal Poly pier ; 5) SLOAPCD Grover Beach site. Ridges extend to between 450 to 550 m (1500-1800 feet) MSL. Base map courtesy of San Luis Obispo County Planning Department, Geographic Technology and Design Section.

Observed sounding, 12 UTC 16 July 2006

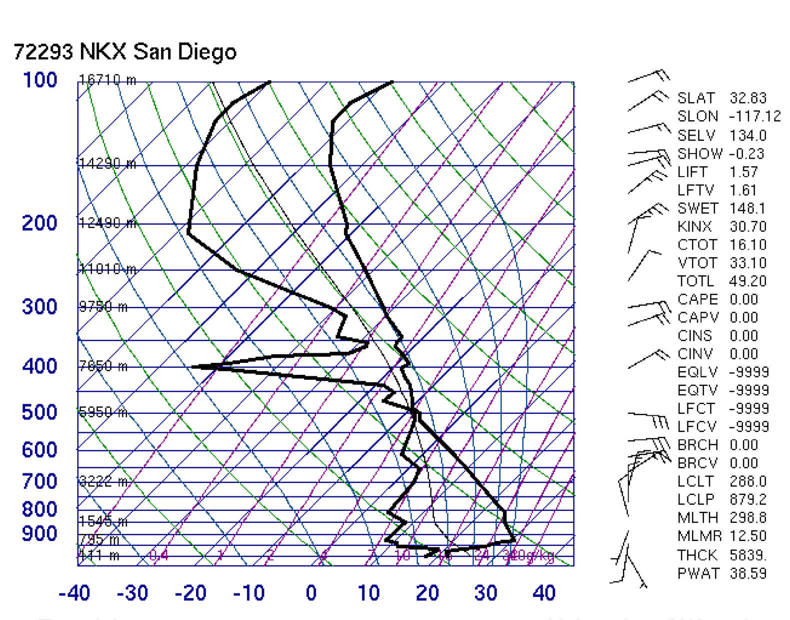

Fig. 3. Observed 12 UTC (05 PDT) sounding from San Diego on July 16 2006. A strong inversion is present over a shallow shallow marine layer. At approximately 550 m, the highest terrain of Santa Cruz Island penetrates the top of the marine layer near 300 m, but does not extend to the top of the inversion layer near 800 m.

The vertical distribution of Froude numbers. within the inversion layer ranges from 0.29 to 0.45, close to the "low Froude number" conditions for eddy formation investigated theoretically by Smolarkiewicz and Rotunno (1989).

Observed sounding, 12 UTC 12 September 2006

Fig. 7 Observed 12 UTC (05 PDT) sounding from San Diego on September 12, 2006. A shallow marine layer is present; the marine layer at the eddy location near Grover Beach is most likely even shallower. Again, the highest terrain penetrates the base of the inversion, but not its top.

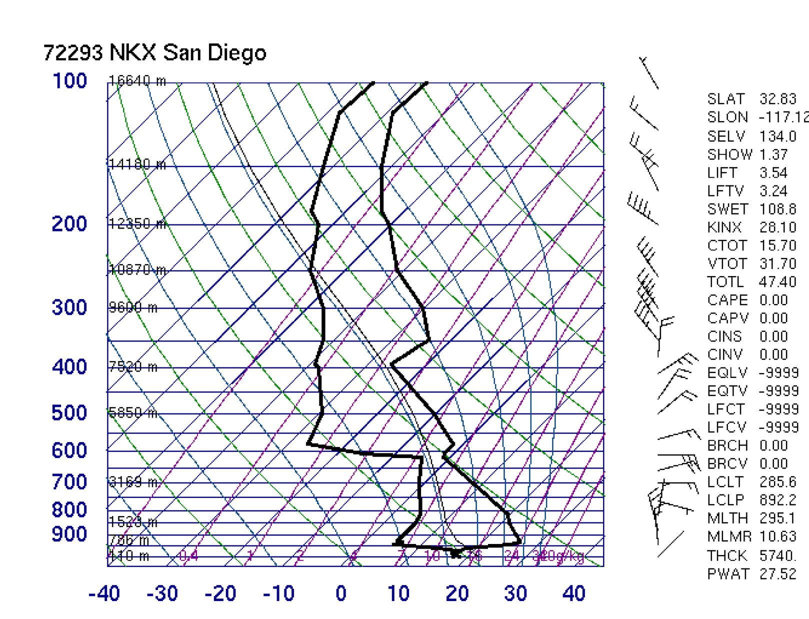

Meteorological Analysis of the Grover Beach Eddy

Diablo Canyon Nuclear Power Plant and its meteorological tower.

Fig. 8. Aerial photographs of PG&E's Diablo Canyon Nuclear Power Plant and surrounding terrain. Left photo: Looking north; 76 m meteorological tower can be seen just to the left of plant. Right photo: looking south. (Courtesy of John Lindsey, Pacific Gas and Electric Company).

Meteogram from PG&E's 76 m meteorological tower at Diablo Canyon Nuclear Power Plant.

Fig. 9 Meteogram during eddy passage

- Dotted curve is temperature (ºC) from 76 m, dashed curve is from 46 m, and the solid curve is from 10 m above ground level (AGL).
- Top row of winds is from 76 m and the bottom row is from 10 m AGL. Half barbs indicate approximately 2.5 ms^{-1} and whole barbs approximately 5 ms^{-1}. Time is in UTC.
- **Temperatures show that eddy has a warm core with the inversion descending to the surface**, providing observational confirmation of theoretical results from Smolarkiewicz and Rotunno (1989) and Schar and Durran (1997) suggesting warm core eddy formation.

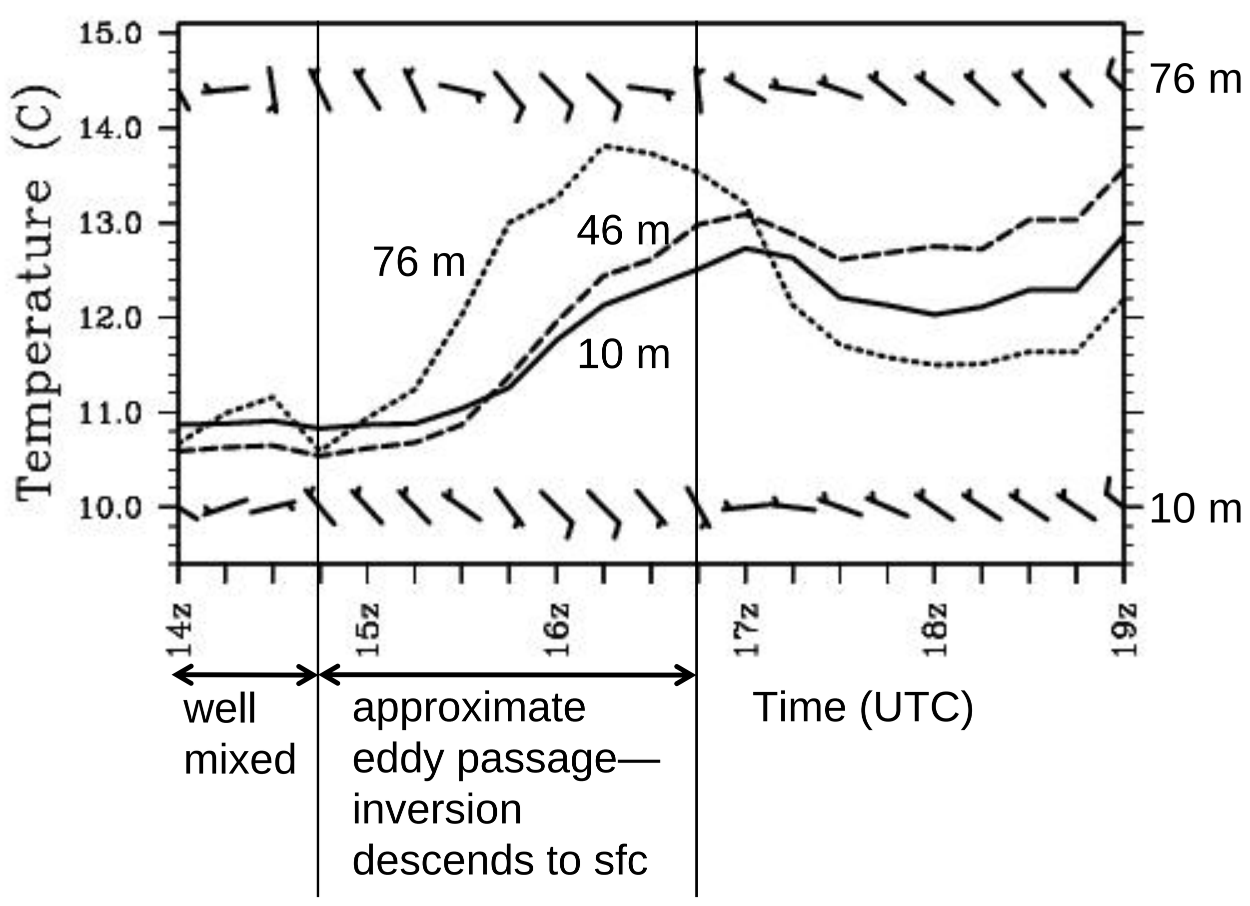

During the eddy passage:
- Temperature trends at 76 m lead those at 10 m by about 45 minutes.
- Cyclonic wind shift at 76 m leads that at 10 m by 15 minutes.
- **Thus, time series suggests that the eddy is leaning forward with height.**

Estimated Froude number Fr for continuously stratified flow at ridgetop level during eddy formation.

$$Fr = \frac{U}{N \cdot h} \qquad (1)$$

$$N = \sqrt{\frac{g}{\theta_v} \cdot \frac{\partial \theta_v}{\partial z}} \qquad (2)$$

where U is the speed of the flow approaching a mountain, h is a characteristic mountain height (taken as 550 m, the height of Davis Peak), and N is the Brunt-Vaisala frequency

Table 1. Froude Number calculations from Equations (1) and (2) where the inversion layer wind from Davis Peak is U. The value in the table represents the average Fr from a mountain-top layer of both the Oakland (KOAK) and San Diego (KNKX) soundings. Since the soundings are from a single time (12 UTC), variations in the estimated Fr are due soley to variations in the Davis Peak wind speed. Values range from 0.35 to 0.45, again, close to the "low Froude number" conditions for eddy formation investigated theoretically by Smolarkiewicz and Rotunno 1989.

Time (UTC)	U (Davis Peak)	Froude Number (Avg. KOAK & KNKX)
1100	5.1	0.35
1115	4.7	0.32
1130	4.9	0.34
1145	5.1	0.35
1200	5.2	0.35
1215	5.1	0.35
1230	4.8	0.33
1245	4.8	0.33
1300	5.5	0.38
1315	5.1	0.36
1330	5.0	0.34
1345	4.9	0.33
1400	5.8	0.40
1415	6.2	0.43
1430	6.5	0.45
1445	6.0	0.41
1500	6.0	0.41

Acknowledgments. This research became possible with much thanks to Skywest pilot Captain Peter Weiss, who originally sent us the eddy photographs, and "KB" who actually photographed the eddies. We gratefully acknowledge John Lindsey and Ed McCarthy of PG&E, Brian Zelenke of Cal Poly, and Gary Arcemont and Joel Craig of San Luis Obispo County Air Pollution Control District. All were instrumental in providing the available meteorological observations. ERAU student Robert Haley provided invaluable assistance in data processing and with some of the figures.

Speculation on eddy formation mechanisms based on the literature of low Froude number (very stable) flow past isolated obstacles:

1. Mechanism 1:

- Based on a synthesis of results from Smolarkiewicz and Rotunno (1989), Rotunno and Smolarkiewicz (1991), Rotunno and Smolarkiewicz (1995), Rotunno et al. (1999), and Epifanio and Durran (2002).
- **Tilting of "backward rolling" (negative) horizontal vorticity into the vertical by vertical velocity differences between strong downslope flow directly in the lee of inversion-penetrating terrain and the weak or non-existent vertical motions on its periphery.**

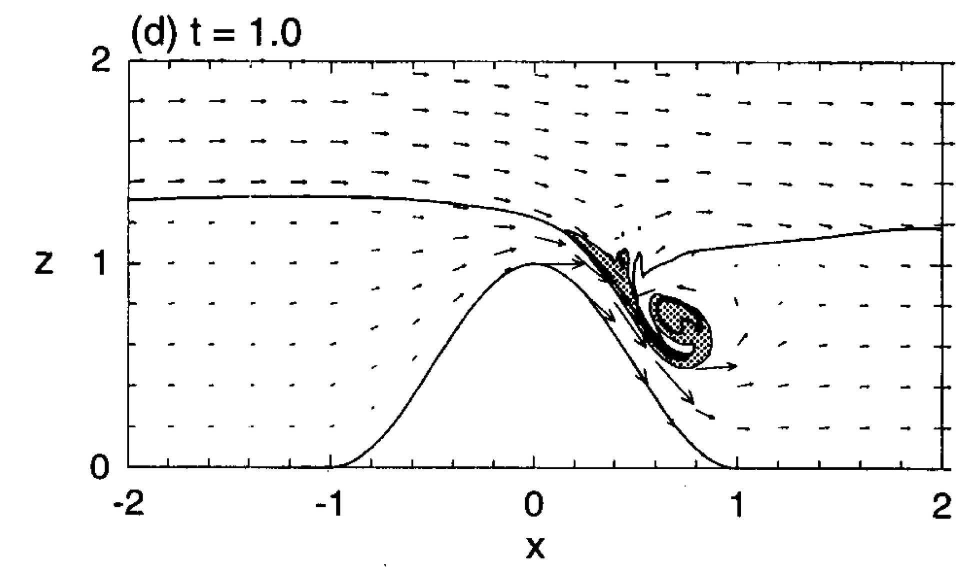

Fig. 10 (from Rotunno and Smolarkiewicz 1995 Figure 3 d). Negative horizontal vorticity (i.e., rotation around a horizontal axis) generated baroclinically by flow along sloping isentropic surfaces, which results in a "backward" (with respect to the mean flow) rolling or overturning motion as the fast moving surface flow undercuts the slower flow above it.

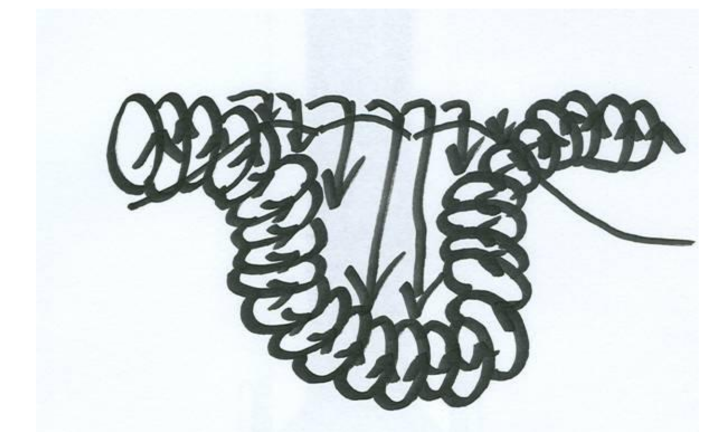

Fig. 11 The "backwards" rolling horizontal vortex tube is tilted into the vertical by the differential vertical velocities between the weak or nonexistent downward motion on the periphery of the high terrain and the maximum downward motion at the terrain centerline (see Figure 3c in Rotunno and Smolarkiewicz 1991) . Viewing upwind against the flow as in this figure, this produces a cyclonically rotating vortex to the left of the centerline..

2. Mechanism 2:

- Based on results of Epifanio and Rotunno (2005) and Schar and Durran (1997) highlighting the role of flow blocking at Froude numbers around 0.3.
- Epifanio and Rotunno (2005) suggest upstream flow-blocking at the lower Froude numbers (greater stability) where more flow tends to go around rather than over an obstacle creates "an adjustment under gravity…caused by the presence of a topographic obstacle moving through the fluid" similar to vortices and flow reversal that might occur at the periphery "produced by a retracting piston in shallow-water theory."

Concluding Remarks on the Grover Beach Eddy

- **Eddy motions and temperature evolution from tower data are consistent with cross-inversion mixing of inversion air down into the marine boundary layer resulting in the cloud-free "eye" feature.**
- **It would not have been possible to resolve the eddy features without the special data obtained for this study from PG&E, the Cal Poly pier, and the San Luis Obispo Air Pollution Control District. No synoptic observing network stations were affected.**
- **Time series of temperature and wind at 76 m vs. 10 m suggests that the eddy is leaning forward with height.**
- **Eddy evolution from satellite imagery is consistent with theoretical results on "low Froude number" flow.**
- **Could eddy formation be a combination of both 1 and 2? Only a detailed model simulation or field study can answer this question.**

References

Epifanio, C. C., and D. R. Durran, 2002b: Lee-vortex formation in free-slip stratified flow over ridges. Part II: Mechanisms of vorticity and PV formation in nonlinear viscous wakes. *J. Atmos. Sci.*, **59**, 1166–1181.

Epifanio, C. C., R. Rotunno, 2005: The dynamics of orographic wake formation in flows with upstream blocking. *J. Atmos. Sci.*, **62**, 3127–3150.

Rotunno, R., and P. K. Smolarkiewicz, 1991: Further results on lee vortices in low-Froude-number flow. *J. Atmos. Sci.*, **48**, 2204–2211.

_____ and _____, 1995: Vorticity generation in the shallow-water equations as applied to hydraulic jumps. *J. Atmos. Sci.*, **52**, 320-330.

_____, V. Grubisic, and _____, 1999: Vorticity and potential vorticity in mountain wakes. *J. Atmos. Sci.*, **56**, 2796-2810.

Schar, C., and D. R. Durran, 1997: Vortex formation and vortex shedding in continuously stratified flows past isolated topography. *J. Atmos. Sci.,* **54,** 534–554.

Smolarkiewicz, P. K., and R. Rotunno, 1989: Low Froude number flow past three-dimensional obstacles. Part I: Baroclinically generated lee vortices. *J. Atmos. Sci.,* **46,** 1154–1164.

Young, G.S., and J. Zawislak, 2006: An observational study of vortex spacing in island wake vortex streets. *Mon. Wea. Rev.*, **134**, 2285-2294.